Hybrid Peptide Helices

DOI: 10.1002/anie.201204436

Structural Characterization of Backbone-Expanded Helices in Hybrid Peptides: $(\alpha\gamma)_n$ and $(\alpha\beta)_n$ Sequences with Unconstrained β and γ Homologues of L-Val**

Krishnayan Basuroy, Bhimareddy Dinesh, Narayanaswamy Shamala, and Padmanabhan Balaram**

Helices and hairpins, ubiquitous elements of secondary structures in proteins, have been targets for synthetic mimetic ("foldamer") design.[1] Foldamer research has intensified following the discovery that polypeptides with homologated (i.e. a backbone with one or more additional $-CH_2-$ groups in the chain), non-natural backbones can readily adopt diverse helical folds.[2] The Pauling α helix is an abundantly observed secondary structure in proteins and is characterized by repetitive 5→1, intramolecular, CO(i)···HN(i+4) 13 atom (C_{13}) hydrogen-bonded rings.[3] The 3_{10} helix is a more tightly wound structure, with repetitive CO(i)···HN(i+3), 10 atom (C_{10}) hydrogen-bonded rings.[4] While the 3_{10} helix is less abundant than the α-helix in proteins, it has been widely characterized in synthetic and natural peptides containing mostly α–α dialkylated residues, primarily α-aminoisobutyric acid (Aib).[5] In polypeptide sequences composed exclusively of α-amino acids $(\alpha\alpha\alpha)_n$, the Pauling α helix incorporates three residues in the hydrogen-bonded turn, while the 3_{10} helix is composed of two residues in the hydrogen-bonded turn. In both cases, only a single set of backbone torsion angles (φ, ψ) characterize an ideal helical structure (α-helix, $\varphi \approx -57.0°$, $\psi \approx -47.0°$; 3_{10} helix, $\varphi \approx -60.0°$, $\psi \approx -30.0°$).[6] Backbone-homologated amino acids, specifically β and γ residues may be incorporated into α amino acid sequences for the generation of helical structures with hybrid backbones.[2,7] For example a regular $(\alpha\beta)_n$ sequence can, in principle, form a regular C_{11} helix, with the αβ segment being the repeating unit resulting in the backbone-expanded analogue of the 3_{10} helix.[8] The three residue $(\alpha\beta\alpha/\beta\alpha\beta)_n$ hydrogen bond repeat, in an $(\alpha\beta)_n$ sequence, would result in a mixed C_{14}/C_{15} helix, which would be a backbone expanded analogue of the α helix.[8a,b,9] Similarly in $(\alpha\gamma)_n$ sequences, the analogue of the 3_{10} helix would be the αγ C_{12} helix,[7e,f,10] while the α helix mimic would be a mixed C_{15}/C_{17} helix.[11] By analogy with studies on α peptides, mixed helical structures with variations in the hydrogen-bonding pattern may also be anticipated. Indeed a growing volume of work on peptides with hybrid backbones suggests that a diversity of hydrogen-bonding patterns can be anticipated.[2,7,8a,11] Thus far, definitive structural characterization of helical structures in hybrid peptides with repeating $(\alpha\beta)_n$ or $(\alpha\gamma)_n$ sequences by X-ray diffraction has been achieved only in the case of stereochemically constrained β and γ residues.[8–10] Constraining backbone atoms by cyclization is a device effectively employed by the Gellman group.[12] The use of geminally disubstituted γ residues, specifically gabapentin, also facilitates folded hydrogen-bonded conformations, permitting crystallographic characterization of hybrid helical structures.[2g,13]

We describe herein the characterization of the αγ C_{12} helix in oligopeptides containing the unconstrained γ residue, $\gamma^4(R)$Val. The structure determination of [Aib-$\gamma^4(R)$Val]$_n$ oligomers ranging in length from four to sixteen residues establishes that C_{12} helices are readily formed. A structural comparison is presented of regular (Aib-Xxx)$_n$ sequences (where, Xxx = α(S)Val, $\beta^3(R)$Val, $\gamma^4(R)$Val) providing insights into the diversity of hydrogen-bonded structures in hybrid molecules (Boc-$\beta^3(R)$Val-OH and Boc-$\gamma^4(R)$Val-OH are formed by homologation of Boc-L-Val-OH (Boc-(S)Val-OH). Note the change in absolute configuration. The abbreviations follow Seebach et al.).[2e]

Figure 1 shows a view of the molecular conformation determined in crystals for the peptides with the sequence Boc-[Aib-$\gamma^4(R)$Val]$_n$-OMe (n = 2,4,5,8). The backbone torsion angles and hydrogen-bond parameters are provided as tables in the Supporting Information. In all cases, successive αγ/γα C_{12} turns are observed, with the number of C_{12} hydrogen bonds as follows: n = 2, 2; n = 4, 6; n = 5, 8; n = 8, 14. Notably, the Aib-$\gamma^4(R)$Val segment adopted very similar conformations in the various peptides permitting determination of the parameters that describe the C_{12} helix. The averaged parameters for the C_{12} helix hydrogen bonds are: N···O (Å) = 2.94 ± 0.07, H···O (Å) = 2.10 ± 0.08, N-H···O (°) = 164.9 ± 7.5. The averaged torsion angles for the C_{12} helical turns are: Aib: φ (°) = −59.4 ± 3.7, ψ (°) = −40.9 ± 4.1; $\gamma^4(R)$Val: φ (°) = −125.4 ± 4.9, θ_1 (°) = 52.6 ± 2.2, θ_2 (°) = 61.2 ± 2.4, ψ (°) = −118.7 ± 6.0. Figure 2 shows a view of an αγ C_{12} turn, which may be viewed as a backbone-expanded analogue of the type-III β turn in an $(\alpha\alpha)_n$ segment. Repetition of the αγ C_{12} turn leads to the C_{12} helix, while repeating the type-III β turn generates the polypeptide

[*] K. Basuroy, Prof. N. Shamala
Department of Physics, Indian Institute of Science,
Bangalore-560 012 (India)
E-mail: shamala@physics.iisc.ernet.in
B. Dinesh, Prof. P. Balaram
Molecular Biophysics Unit, Indian Institute of Science
Bangalore-560 012 (India)
E-mail: pb@mbu.iisc.ernet.in

[**] This work is supported by a program grant from the Department of Biotechnology (DBT), India, in the area of Molecular Diversity and Design. B.D. is supported by the award of a UGC-DSK Postdoctoral Fellowship from the University Grants Commission (UGC), India.

Supporting information for this article is available on the WWW under http://dx.doi.org/10.1002/anie.201204436.

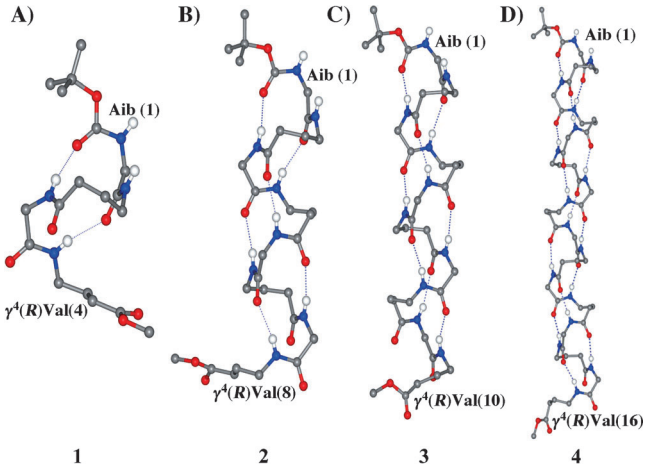

Figure 1. Conformation in crystals of peptides: A) Boc-[Aib-γ^4(*R*)Val]$_2$-OMe (**1**), B) Boc-[Aib-γ^4(*R*)Val]$_4$-OMe (**2**), C) Boc-[Aib-γ^4(*R*)Val]$_5$-OMe (**3**), and D) Boc-[Aib-γ^4(*R*)Val]$_8$-OMe (**4**). Side chains are not shown for clarity. C = gray; H = white; O = red; N = blue.

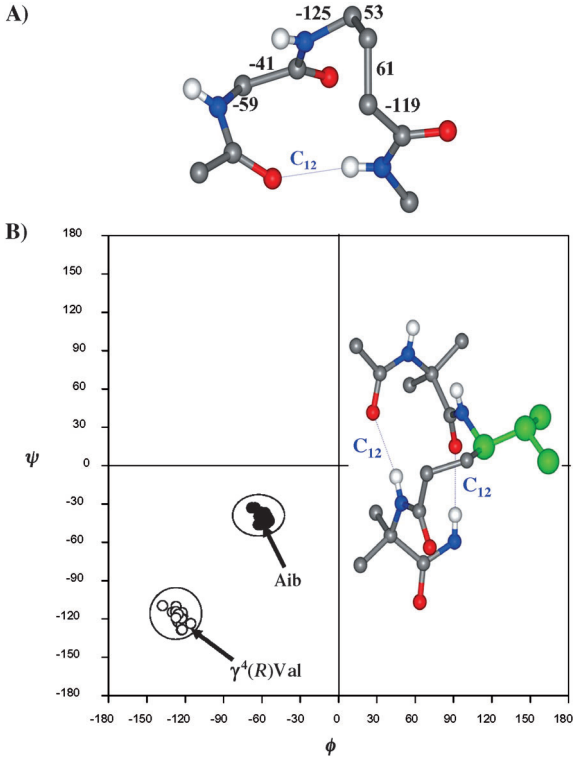

Figure 2. A) Average backbone torsion angles for an αγ C_{12} helical turn in Boc-[Aib-γ^4(*R*)Val]$_n$-OMe peptides (**1**–**4**), B) φ, ψ cluster plot for Aib and γ^4(*R*)Val residues in C_{12} helices. Inset: view of a turn of a C_{12} helix highlighting the position of the γ^4(*R*)Val residue (green). C = gray; H = white; O = red; N = blue.

3_{10} helix. In all cases, the γ^4(*R*)Val residue adopted the *gauche–gauche* conformation about the C^γ–C^β (θ_1) and C^β–C^α (θ_2) bonds (θ_1 (°) = 52.6 ± 2.2, θ_2 (°) = 61.2 ± 2.4). The distribution of the torsion angles about the N–C^γ (φ) and C^α–CO (ψ) bonds is also shown in Figure 2. An incipient C_{12}-helical structure, with two consecutive C_{12}-hydrogen bonds has been characterized recently in crystals of the tetrapeptide Boc-Aib-γ^4Phe-Aib-γ^4Phe-OEt.[14]

The configuration of the C_{12} helix in the αγ sequence described above prompted us to compare the analogous $(\alpha\alpha)_n$ and $(\alpha\beta)_n$ sequences. Figure 3 and Figure 4 show the molecular conformations determined in crystals for the tetrapeptides Boc-[Aib-α(*S*)Val]$_2$-OMe, Boc-[Aib-β^3(*R*)Val]$_2$-OMe,

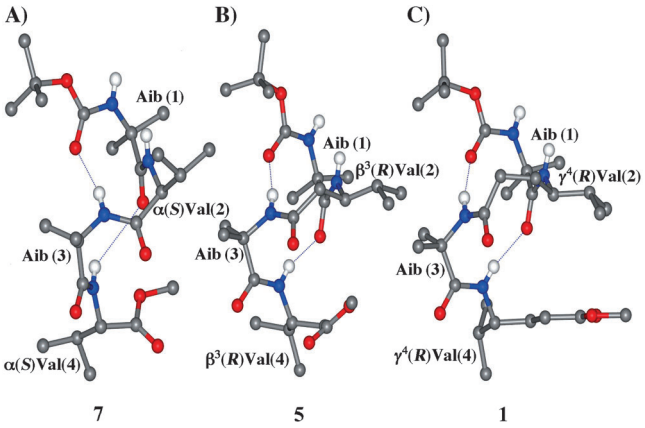

Figure 3. Conformation in crystals of tetrapeptides: A) Boc-[Aib-α(*S*)Val]$_2$-OMe (**7**), B) Boc-[Aib-β^3(*R*)Val]$_2$-OMe (**5**), C) Boc-[Aib-γ^4(*R*)Val]$_2$-OMe (**1**). C = gray; H = white; O = red; N = blue.

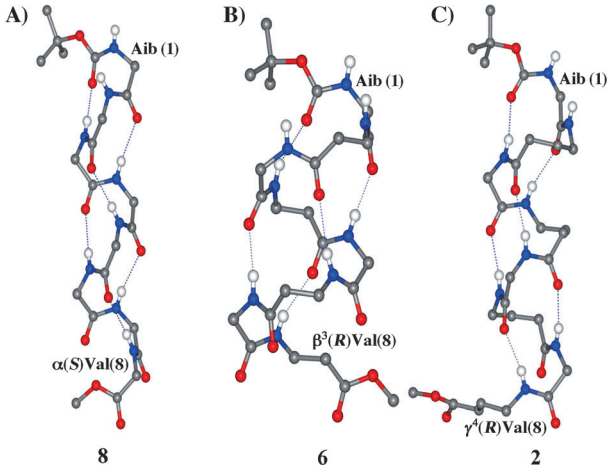

Figure 4. Conformation in crystals of octapeptides: A) Boc-[Aib-α(*S*)Val]$_4$-OMe (**8**), B) Boc-[Aib-β^3(*R*)Val]$_4$-OMe (**6**), C) Boc-[Aib-γ^4(*R*)Val]$_4$-OMe (**4**). Side chains are not shown for clarity. C = gray; H = white; O = red; N = blue.

and Boc-[Aib-γ^4(*R*)Val]$_2$-OMe and the octapeptides Boc-[Aib-α(*S*)Val]$_4$-OMe, Boc-[Aib-β^3(*R*)Val]$_4$-OMe, and Boc-[Aib-γ^4(*R*)Val]$_4$-OMe (where α(*S*)Val = L-Val). The structures of the three tetrapeptides reveal two C_{10} hydrogen bonds corresponding to formation of one 3_{10} helical turn in the case of Boc-[Aib-α(*S*)Val]$_2$-OMe, as anticipated. The corresponding β and γ analogues reveal the formation of two consecutive C_{11} and C_{12} turns, respectively. Upon lengthening the oligopeptide sequences to octapeptides, clear differences in the intramolecular hydrogen-bonding patterns emerge. The $(\alpha\alpha)_n$ sequence in Boc-[Aib-α(*S*)Val]$_4$-OMe shows six successive C_{10} hydrogen bonds corresponding to an almost ideal

3_{10} helical structure.[15] Backbone torsion angles and hydrogen-bond parameters are provided as tables in the Supporting Information. As already noted, the $(\alpha\gamma)_4$ sequence yields a perfect C_{12} helix. In sharp contrast, the $(\alpha\beta)_4$ sequence yields a mixed C_{14}/C_{15} helix, with the formation of three C_{14} ($\alpha\beta\alpha$) and two C_{15} ($\beta\alpha\beta$) hydrogen bonds. In this case, the repetitive units are three-residue hydrogen-bonded turns formed by CO(i)···HN(i+4) interactions, analogous to that observed in the classical α-helix.

Table 1: Peptide sequences and relevant physical parameters.

Peptides (No.)	Melting point [°C]	ESI-MS [Da] $[M+H]^+$, $[M+Na]^+$, $[M+K]^+$	M_{cal}	Space group
Boc-[U[a]-$\gamma^4(R)$V[b]]$_2$-OMe (**1**)	162–164	557.2, 579.2, 595.1	556.3	$P2_1$
Boc-[U-$\gamma^4(R)$V]$_4$-OMe (**2**)	232–234	981.1, 1003.1, 1019.0	980.7	$P2_12_12_1$
Boc-[U-$\gamma^4(R)$V]$_5$-OMe (**3**)	251–252	1193.0, 1215.0, 1230.9	1192.8	$P2_1$
Boc-[U-$\gamma^4(R)$V]$_8$-OMe (**4**)	[c]	1829.7, 1851.7, 1867.6	1829.3	$P2_12_12_1$
Boc-[U-$\beta^3(R)$V]$_2$-OMe (**5**)	195–197	529.2, 551.1, 567.1	528.3	$P2_1$
Boc-[U-$\beta^3(R)$V]$_4$-OMe (**6**)	242–243	925.0, 947.0, 962.9	924.6	$P2_12_12_1$
Boc-[U-$\alpha(S)$V]$_2$-OMe (**7**)	151–152	501.2, 523.2, 539.1	500.3	$P2_12_12_1$
Boc-[U-$\alpha(S)$V]$_4$-OMe (**8**)	240–241	861.0, 891.0, 907.0	868.6	$P2_1$

[a] U = Aib. [b] V = Val. [c] Did not melt up to 300 °C.

Two factors undoubtedly contribute to the stability of oligopeptide helices. First, the number of intramolecular hydrogen bonds formed over the length of the peptide must favor the tighter helices formed by repetitive turns with fewer atoms in the hydrogen-bonded ring. For example, the 3_{10} helix might be expected to be favored over the α helices in short peptides. Indeed a study of mixed α/β (1:1) sequences has revealed a pronounced chain-length dependence of helix type.[8b] With increasing chain length, the differences in the hydrogen-bonding contribution diminish. Second, α helix stability must be strongly influenced by non-bonded interactions, with large diameter helices being disfavored by poor internal packing. It may be predicted that repetition of large hydrogen-bonded rings will lead to suboptimally packed helix interiors. Indeed the π helix in α peptides, which incorporates a repetitive C_{16} hydrogen-bonded ring, is rarely found in peptides and proteins.[2g,16] In hybrid sequences containing backbone-homologated residues, this interplay of hydrogen bonds and van der Waals interactions in the helix interior may determine the nature of the structures found. The results presented herein clearly demonstrate that in $(\alpha\gamma)_n$ sequences the C_{12} hydrogen-bonding pattern is favored almost exclusively. The larger C_{15} hydrogen-bonding pattern, which may be predicted for the three-residue αγα repeat, is not found in the [Aib-$\gamma^4(R)$Val]$_n$ series. The C_{17} hydrogen-bonded turn predicted for the γαγ segment is also not found.

The comparison of the Boc-[Aib-Xxx]$_4$-OMe octapeptides suggests that greater heterogeneity of helix type may be expected in the $(\alpha\beta)_n$ sequences, as compared to the $(\alpha\gamma)_n$ sequences. These studies with the unconstrained γ residue $\gamma^4(R)$Val suggest that hybrid sequences incorporating the readily accessible γ residues, which are backbone homologues of the α amino acids found in proteins, may be used effectively in generating stable mimetics of folded structures found in proteins and biologically active peptides.

Experimental Section

Table 1 lists the sequences and relevant physical parameters determined for each of the peptides in this study. The amino acids, Boc-$\gamma^4(R)$Val-OH and Boc-$\beta^3(R)$Val-OH were synthesized by previously described procedures.[2b,17] All the peptides were prepared by solution-phase synthesis using the *tert*-butyloxycarbonyl (Boc) group for N terminal protection. The C terminus was protected using a methyl ester. Deprotections were performed using 98% formic acid and 1:1 trifluoroacetic acid:dichloromethane (TFA:DCM) to remove the Boc group, whereas the methyl ester was removed by alkaline hydrolysis. Couplings were mediated by isobutylchloroformate (IBCF) and 1-hydroxy-1H-benzotriazole (HOBt; 1.01 equiv) for dipeptides and the successive peptides with *O*-(7-azabenzotriazol-1-yl)-*N*,*N*,*N*′,*N*′-tetramethyluronium hexafluorophosphate (HATU) and HOBt. All intermediates were characterized by electrospray ionization mass spectrometry (ESI-MS), 500/700 MHz ^{1}H NMR spectroscopy, and thin-layer chromatography (TLC) on silica gel (SiO_2, $CHCl_3$/MeOH 9:1 (*v*/*v*)) and were used without further purification. The final peptides were obtained as pure products after washing with hexane–ether mixtures. The peptide **4** was purified by stirring with methanol and filtering through a sintered glass crucible. Purity of the final peptides was assessed using reversed-phase high-performance liquid chromatography (HPLC) on a C_{18} column (5–10 μm, 7.8–250 mm) using methanol/water systems and monitored at 226 nm. The peptides were characterized by ESI-MS and 700 MHz ^{1}H NMR spectroscopy.

X-ray diffraction datasets were collected using $Cu_{K\alpha}$ (1.54178 Å) radiation for peptides **1**, **2**, **3**, **4**, and **8** and $Mo_{K\alpha}$ (0.71073 Å) radiation for peptides **5**, **6**, and **8**, using BRUKER AXS SMART APEXII ULTRA CCD (rotating anode X-ray generator) and BRUKER AXS KAPPA APEXII CCD diffractometer respectively. Data collection was carried out in phi and omega scan-type mode using dry crystals at 296 K for peptides **1**, **3**, **4**, **5**, **6**, **7**, and **8**. Crystals of peptide **2** were fragile and data was collected using a glass capillary with mother liquor (dichloromethane) at 296 K. For peptide **3**, data collection was carried out at low temperature (240 K) to resolve the positional disorder (i.e. whether it is static or dynamic) of the $\gamma^4(R)$Val(8) side chain, which turned out to be positional static disorder. All peptide structures were solved using iterative dual-space direct methods in SHELXD.[18] After the initial solution methods, all the structures were refined against F^2 isotropically followed by full-matrix anisotropic least-squares refinement using SHELXL-97.[19] The high quality of the diffraction data enabled location of many H atoms in these peptides directly from the difference Fourier map. All H atoms attached to backbone N atoms could be located in peptides **1**, **2**, **3**, **4**, **6**, and **8**. In peptide **5**, all the hydrogen atoms were fixed geometrically in idealized positions and allowed to ride on the C or N atoms to which they were bonded, in the final cycles of refinement. In tetrapeptide **7**, only five hydrogen atoms attached to the atoms N1, N2, C4A, C2A, and C4B were located from the difference Fourier map. Positional disorder in peptides **3, 4** (in $\gamma^4(R)$Val(8) side chain), and **2** (in co-crystallized solvent) was treated with PART commands and also with proper restraints and constraints to obtain chemically meaningful geometry of the disordered groups. Apart from tetrapeptide **5**, the remaining hydrogen atoms, other than those which were located from difference Fourier map, were fixed geometrically in the idealized position and allowed to ride on the C or N atoms to which they were bonded, in the final cycles of refinement. The details of the

crystal data and structure refinement for all the peptides mentioned above are provided as tables in the Supporting Information.

CCDC deposition numbers for the peptides are 881181 (**1**), 881182 (**2**), 881177 (**3**), 881178 (**4**), 881179 (**5**), 881180 (**6**), 881183 (**7**), and 882909 (**8**) and contain the supplementary crystallographic data for this paper. These data can be obtained free of charge from The Cambridge Crystallographic Data Centre via www.ccdc.cam.ac.uk/data_request/cif.

Received: June 7, 2012
Published online: July 25, 2012

Keywords: backbone conformations · helices · hybrid peptides · hydrogen bonds · X-ray diffraction

[1] a) S. H. Gellman, *Acc. Chem. Res.* **1998**, *31*, 173 – 180; b) J. Venkatraman, S. C. Shankaramma, P. Balaram, *Chem. Rev.* **2001**, *101*, 3131 – 3152.

[2] a) D. H. Appella, L. A. Christianson, D. A. Klein, D. R. Powell, L. Huang, J. J. Barchi, S. H. Gellman, *Nature* **1997**, *387*, 381 – 382; b) D. Seebach, M. Overhand, F. M. N. Kuhnle, B. Martinoni, L. Oberer, U. Hommel, H. Widmer, *Helv. Chim. Acta* **1996**, *79*, 913 – 941; c) D. Seebach, M. Brenner, M. Rueping, B. Schweizer, B. Jaun, *Chem. Commun.* **2001**, 207 – 208; d) R. P. Cheng, S. H. Gellman, W. F. DeGrado, *Chem. Rev.* **2001**, *101*, 3219 – 3232; e) D. Seebach, A. K. Beck, D. J. Bierbaum, *Chem. Biodiversity* **2004**, *1*, 1111 – 1239; f) D. Seebach, J. Gardiner, *Acc. Chem. Res.* **2008**, *41*, 1366 – 1375; g) P. G. Vasudev, S. Chatterjee, N. Shamala, P. Balaram, *Chem. Rev.* **2011**, *111*, 657 – 687; h) F. Bouillère, S. Thétiot-Laurent, C. Kouklovsky, V. Alezra, *Amino Acids* **2011**, *41*, 687 – 707; i) D. H. Appella, L. A. Christianson, I. L. Karle, D. R. Powell, S. H. Gellman, *J. Am. Chem. Soc.* **1996**, *118*, 13071 – 13072.

[3] a) L. Pauling, R. B. Corey, H. R. Branson, *Proc. Natl. Acad. Sci. USA* **1951**, *37*, 205 – 211; b) L. Pauling, R. B. Corey, *Proc. Natl. Acad. Sci. USA* **1951**, *37*, 729 – 740.

[4] J. Donohue, *Proc. Natl. Acad. Sci. USA* **1953**, *39*, 470 – 478.

[5] a) B. V. Venkataram Prasad, P. Balaram, E. Benedetti, *CRC Crit. Rev. Biochem.* **1984**, *16*, 307 – 348; b) I. L. Karle, P. Balaram, *Biochemistry* **1990**, *29*, 6747 – 6756; c) C. Toniolo, E. Benedetti, *Macromolecules* **1991**, *24*, 4004 – 4009; d) S. Aravinda, N. Shamala, R. S. Roy, P. Balaram, *Proc. Indian Acad. Sci. Chem. Sci.* **2003**, *115*, 373 – 400; e) C. Toniolo, M. Crisma, F. Formaggio, C. Peggion, *Biopolymers* **2001**, *60*, 396 – 419.

[6] G. N. Ramachandran, V. Sasisekharan, *Adv. Protein Chem.* **1968**, *23*, 283 – 437.

[7] a) I. L. Karle, A. Pramanik, A. Bannerjee, S. Bhattacharya, P. Balaram, *J. Am. Chem. Soc.* **1997**, *119*, 9087 – 9095; b) W. S. Horne, S. H. Gellman, *Acc. Chem. Res.* **2008**, *41*, 1399 – 1408; c) S. Chatterjee, R. S. Roy, P. Balaram, *J. R. Soc. Interface* **2007**, *4*, 587 – 606; d) R. S. Roy, I. L. Karle, S. Raghothama, P. Balaram, *Proc. Natl. Acad. Sci. USA* **2004**, *101*, 16478 – 16482; e) K. Ananda, P. G. Vasudev, A. Sengupta, K. M. P. Raja, N. Shamala, P. Balaram, *J. Am. Chem. Soc.* **2005**, *127*, 16668 – 16674; f) P. G. Vasudev, K. Ananda, S. Chatterjee, S. Aravinda, N. Shamala, P. Balaram, *J. Am. Chem. Soc.* **2007**, *129*, 4039 – 4048.

[8] a) C. Baldauf, R. Günther, H. J. Hofmann, *Biopolymers* **2006**, *84*, 408 – 413; b) S. H. Choi, I. A. Guzei, L. C. Spencer, S. H. Gellman, *J. Am. Chem. Soc.* **2008**, *130*, 6544 – 6650; c) M. A. Schmitt, S. H. Choi, I. A. Guzei, S. H. Gellman, *J. Am. Chem. Soc.* **2005**, *127*, 13130 – 13131; d) M. A. Schmitt, S. H. Choi, I. A. Guzei, S. H. Gellman, *J. Am. Chem. Soc.* **2006**, *128*, 4538 – 4539; e) S. H. Choi, I. A. Guzei, L. C. Spencer, S. H. Gellman, *J. Am. Chem. Soc.* **2009**, *131*, 2917 – 2924; f) W. S. Horne, J. L. Price, J. L. Keck, S. H. Gellman, *J. Am. Chem. Soc.* **2007**, *129*, 4178 – 4180.

[9] S. H. Choi, I. A. Guzei, S. H. Gellman, *J. Am. Chem. Soc.* **2007**, *129*, 13780 – 13781.

[10] a) S. Chatterjee, P. G. Vasudev, S. Ragothama, N. Shamala, P. Balaram, *Biopolymers* **2008**, *90*, 759 – 771; b) S. Chatterjee, P. G. Vasudev, S. Ragothama, C. Ramakrishnan, N. Shamala, P. Balaram, *J. Am. Chem. Soc.* **2009**, *131*, 5956 – 5965; c) L. Guo, Y. Chi, A. M. Almeida, I. A. Guzei, B. K. Parker, S. H. Gellman, *J. Am. Chem. Soc.* **2009**, *131*, 16018 – 16020.

[11] C. Baldauf, R. Günther, H. J. Hofmann, *J. Org. Chem.* **2006**, *71*, 1200 – 1208.

[12] a) D. H. Appella, L. A. Christianson, D. A. Klein, M. R. Richards, D. R. Powell, S. H. Gellman, *J. Am. Chem. Soc.* **1999**, *121*, 7574 – 7581; b) L. Guo, W. Zhang, A. G. Reidenbach, W. M. Giuliano, I. A. Guzei, L. C. Spencer, S. H. Gellman, *Angew. Chem.* **2011**, *123*, 5965 – 5968; *Angew. Chem. Int. Ed.* **2011**, *50*, 5843 – 5846.

[13] P. G. Vasudev, S. Chatterjee, N. Shamala, P. Balaram, *Acc. Chem. Res.* **2009**, *42*, 1628 – 1639.

[14] A. Bandyopadhyay, H. N. Gopi, *Org. Lett.* **2012**, *14*, 2770 – 2773.

[15] S. Aravinda, S. Datta, N. Shamala, P. Balaram, *Angew. Chem.* **2004**, *116*, 6896 – 6899; *Angew. Chem. Int. Ed.* **2004**, *43*, 6728 – 6731.

[16] R. N. Chapman, J. L. Kulp III, A. Patgiri, N. R. Kallenbach, C. Bracken, P. S. Arora, *Biochemistry* **2008**, *47*, 4189 – 4195.

[17] a) K. Pluncińska, B. Liberek, *Tetrahedron* **1987**, *43*, 3509 – 3517; b) C. Guibourdenche, D. Seebach, *Helv. Chim. Acta* **1997**, *80*, 1 – 13; c) M. Smrcina, P. Majer, E. Majerova, T. A. Guerassina, M. A. Eissenstat, *Tetrahedron* **1997**, *53*, 12867 – 12874; d) B. Dinesh, K. Basuroy, N. Shamala, P. Balaram, *Tetrahedron* **2012**, *68*, 4374 – 4380.

[18] T. R. Schneider, G. M. Sheldrick, *Acta Crystallogr. D* **2002**, *D58*, 1772 – 1779.

[19] a) G. M. Sheldrick, SHELXL-97, A Program for Crystal Structure Refinement; University of Göttingen: Göttingen, **1997**; b) G. M. Sheldrick, *Acta Crystallogr. A* **2008**, *A64*, 112 – 122.

